Available online at www.sciencedirect.com
SCIENCE DIRECT®
Journal of Magnetic Resonance 173 (2005) 75–83
JMR Journal of Magnetic Resonance
www.elsevier.com/locate/jmr

^{1}H NMRD profiles and ESR lineshapes of Gd(III) complexes: a comparison between the generalized SBM and the stochastic Liouville approach

Xiangzhi Zhou, Per-Olof Westlund*

Department of Biophysical Chemistry, Umeå University, SE-901 87 Umeå, Sweden

Received 15 September 2004; revised 26 October 2004
Available online 15 December 2004

Abstract

A complete description of the T_1-NMRD profiles and the ESR lineshape of Gd(III) complexes ($S = 7/2$) was presented using second-order perturbation theory (GSBM) by Zhou et al. [J. Magn. Reson. 167 (2004) 147]. This report compares the GSBM with the stochastic Liouville approach (SLA) to determine the validity of the closed analytical expressions of NMRD and the ESR lineshape functions. Both approaches give the same results at high fields while a very small divergence is observed for X- and W-band ESR lineshapes when the magnitude of the perturbation term times the correlation time approaches the limit of the perturbation regime, $\Delta_{ZFS}\tau_f \approx 0.1$. There was a clear discrepancy between the theoretical GSBM X-band spectrum and the recorded ESR spectrum of the Gd(III) MS-325 + HSA complex. This is probably due to a slow-motion effect caused by a slow modulation of the ZFS interaction. The characteristic correlation time of this slow modulation is in the range of 150 ps, which therefore cannot be due to the reorientational motion of the whole MS-325 + HSA complex.

Keywords: GSBM; SLA; NMRD; ESR; MS-325

1. Introduction

Paramagnetic relaxation enhancement (PRE) is a phenomenon that usually explains the enhancement of water proton spin–lattice relaxation in the presence of paramagnetic ions. The PRE influences are very important in MRI studies because they are responsible for contrasting effects in the generated images [1]. The original Solomon–Bloembergen–Morgan (SBM) theory [2–4] has been widely used to describe this phenomenon. The SBM theory is condensed into simple mathematical expressions, which makes it easy to apply in the analyses of experimental data. SBM is a second-order perturbation theory, which is only valid in the high-field regime, where the Zeeman Hamiltonian is much larger than the perturbation Hamiltonian [5]. Furthermore, for high-spin metal ions ($S > 1$), the SBM theory is only valid for the electron spin system in the extreme narrowing regime. Consequently, it does not account for multiple exponential electron spin relaxation and dynamic frequency shifts [6,7].

Recently, we have developed a generalized SBM theory (GSBM) which fully includes multi-exponential electron spin relaxation as well as the dynamic frequency shift [8–10]. GSBM may be expressed in a closed analytical form, but the expressions are somewhat more complicated than the SBM expressions. In addition, the complete ESR lineshape function $I(\omega)$ is derived within the same spin Hamiltonian model as in GSBM. GSBM thus simplifies a combined ESR and NMRD-PRE analysis of Gd(III) complexes [10]. The GSBM has been implemented into a simple Fortran program, which should be a useful tool for experimental analysis of both

* Corresponding author.
E-mail address: per-olof.westlund@chem.umu.se (P.-O. Westlund).

1090-7807/$ - see front matter © 2004 Published by Elsevier Inc.
doi:10.1016/j.jmr.2004.10.014

T_1-NMRD profiles and ESR experiments (all available ESR bands). A combined NMRD and ESR analysis has also been recommended by other research groups, using an approach which includes a direct simulation method of the electron spin relaxation [11–14]. This approach may treat the non-perturbation regime as well but thus demands more computational power. Fries, Rast, and co-workers [11–14] have analysed the ESR spectra of several Gd(III) complexes and found that both a static and a transient zero-field splitting (ZFS) are needed. The accuracy of a second-order perturbation theory is questionable for slow tumbling complexes with a static zero-field splitting interaction. The influence on ESR spectra of fourth- and sixth-order terms of the ZFS interaction has been studied as well [13]. In principle, it is straightforward to include these higher-order terms of the ZFS interaction in our approach. One must determine the corresponding Redfield relaxation elements and include them in the Relaxation matrix (cf. Appendix A, Eq. (A.1)). However, an extension of the ZFS Hamiltonian to higher rank terms introduces extra parameters, which should be determined. This is a difficult matter. The estimation of fourth and sixth rank parameters, made by Rast et al. [13], and based on multi-frequency ESR linewidth analysis, is not conclusive. Their fourth-order parameter is of the same size as their sixth rank parameter. However, one may expect that the sixth rank parameter should be smaller than the fourth rank parameter. An alternative view is to regard the inclusion of high rank ZFS terms, as a way of mimicking a complex dynamics model of the ZFS correlation function. The reorientational correlation times of higher rank tensors introduce spectral density functions with several dispersions, determined by the correlation times $\tau 2 = 140/6$, $\tau 4 = 140/20$, and $\tau 6 = 140/42$ ps, where $\tau_L = \tau_R/L(L+1)$. The ZFS correlation function is essentially unknown and a single exponential decay is clearly a simplification. The intermediate, or low-field limit regime, may also influence X-band ESR spectra, but this effect has not previously been studied. It is therefore motivated to investigate the regime of validity of the relatively simple GSBM theory as well as to produce the characteristic NMRD profiles and X or any higher frequency band ESR lineshapes for regimes where the GSBM may be questionable.

In this work, we compare the NMRD and ESR results obtained using the stochastic Liouville approach (SLA) with the corresponding GSBM results. This is carried out using the simple pseudo-rotation model [15] using only a ZFS parameter and a distortion correlation time τ_f. For a comparison between SLA and GSBM, this is sufficient because the crucial factor, determining the applicability of the perturbation theory (GSBM), is the interaction factor defined as Δ_{ZFS} (the ZFS interaction strength) $\times \tau_f$. The SLA gives a complete relaxation description of the electron spin systems, whereas the nuclear spin system is described in the perturbation regime. The low-field regime, where the ZFS interaction is larger than the Zeeman interaction, is also fully described. For the interested reader we recommend comprehensive review articles in this field [16,17]. The SLA has most often been applied to $S = 1$ where more details are given about how to set up the Liouville matrix [17–19].

In this work, we present evidence that the X-band spectrum of Gd(III) complex MS-325 in the presence of human serum albumin (HSA) displays the non-Lorentzian character because there is a slowly modulated ZFS interaction. However, this modulation is too fast to be due to the reorientational tumbling of the whole complex.

This paper is organized as follows: First, we give a brief review of the NMR-PRE theory, focusing on the GSBM and SLA approaches. Then, we present and discuss a couple of cases where GSBM and SLA may be expected to generate different results. The analysis of the MS-325 complex associated with HSA is interesting because the X-band spectra could not be described within the GSBM theory, whereas the NMRD profile was well described [10]. In Appendices A and B, we give the full expressions of the GSBM theory and in Appendix C the complex ESR lineshape function is presented. These expressions have not previously been published. A computer program is written in Fortran and may be obtained upon request from Xiangzhi.Zhou@chem.umu.se.

2. Theory

The inner sphere water proton relaxivity, $R_1 = 1/T_{1p}[M]$, is expressed as the relaxation enhancement divided by the concentration of paramagnetic ions, measured in units of $(\frac{\text{mmol}}{\text{dm}^3}\text{s})^{-1}$. The relaxivity R_1 produces the NMRD profile when measured as a function of the nuclear Larmor frequency ω_I.

$$\frac{1}{T_{1p}[M]} = \left(\frac{2q \cdot 10^{-3}}{55.56}\right)\frac{1}{T_{1M} + \tau_M}. \tag{1}$$

Here, q denotes the number of fast exchanging water molecules in the first hydration shell of a paramagnetic metal ion with electron spin quantum number S. The concentration of paramagnetic ions is denoted $[M]$ and for water it is 55.56 $\frac{\text{mol}}{\text{dm}^3}$. The mean life time for the inner water sphere is denoted τ_M. T_{1M} is the spin–lattice relaxation time of inner sphere water molecules. In this work, all model calculations are made under fast exchange conditions $\tau_M \ll T_{1M}$. Considering only the relaxation contribution due to nuclear spin–electron spin dipole–dipole interaction, the paramagnetic enhanced proton spin–lattice relaxation time T_{1M} is given by

$$\frac{1}{T_{1M}} = \frac{4}{3}\left(\frac{\mu_0}{4\pi}\right)^2 \hbar^2 \gamma_I^2 \gamma_S^2 \frac{S(S+1)}{r_{IS}^6}\tau_c^{\text{DD}}. \tag{2}$$

Here, μ_0, $\hbar$, γ_I, and γ_S have their usual physical meanings and the effective electron spin–nuclear spin dipole–dipole correlation time τ_c^{DD} is defined as,

$$\tau_c^{\mathrm{DD}} = \mathrm{Re}(0.1 \times s_1^{\mathrm{DD}} + 0.3 \times s_0^{\mathrm{DD}} + 0.6 \times s_{-1}^{\mathrm{DD}}), \tag{3}$$

which is a weighted sum of spectral density functions s_σ^{DD}, where σ can take the values -1, 0, and $+1$. The spectral density s_σ^{DD} is the Fourier–Laplace transform of the reorientation correlation function and the electron spin correlation function, $\mathrm{tr}_S\{S_\sigma^{1\dagger} e^{i\mathcal{L}_S\tau} S_\sigma^1 \rho_S^T\}$, at the nuclear Larmor frequency ω_I.

$$\begin{aligned} s_\sigma^{\mathrm{DD}}(\omega_I + \sigma\omega_S) &= \frac{3}{S(S+1)} \\ &\quad \times \int_0^\infty \mathrm{tr}_S\left\{S_\sigma^{1\dagger} e^{i\mathcal{L}_S\tau} S_\sigma^1 \rho_S^T\right\} e^{-(i\omega_I + 1/\tau_R)\tau}\, d\tau \\ &\equiv M_{\sigma\sigma}^{-1}. \end{aligned} \tag{4}$$

Two assumptions are used in the derivation of Eq. (4). First, the complete electron spin dipole–nuclear spin dipole correlation function [16,17] has been decomposed into a pure reorientational and an electron spin correlation function. This is strictly valid, provided the electron spin relaxation is independent of the reorientation modulated electron spin relaxation mechanism [17]. Second, the reorientational correlation function is taken to be isotropic and characterized by one reorientational correlation time τ_R. Thus, the important quantity is the electron spin correlation function, which is given by $\langle S_\sigma^{1\dagger}(t) S_\sigma^1(0)\rangle \equiv \mathrm{tr}_S\{S_\sigma^{1\dagger} e^{i\mathcal{L}_S\tau} S_\sigma^1 \rho_S\}$. The connection between NMRD-PRE and ESR lineshape experiments is thus evident. The latter focuses on the complex lineshape function $I(\omega - \omega_S)$,

$$\begin{aligned} I(\omega - \omega_S) &= \int_0^\infty e^{-i\omega t}\, \mathrm{tr}_S\left\{S_1^{1\dagger} e^{i\hat{L}_S\tau} S_1^1 \rho_S^T\right\} dt \\ &\equiv \alpha\tilde{\rho}_1^1(\omega - \omega_S), \end{aligned} \tag{5}$$

whose real and imaginary parts represent the absorption spectrum and the dispersion spectrum, respectively. Here, ω_S denotes the electron Larmor frequency and $\mathcal{L}_S$ is the Liouville operator which governs the time dependence of the electron spin correlation function (cf. Eq. (6)). The ESR lineshape is obtained as the derivative of the absorption spectra (i.e., $\mathrm{Re}\, I(\omega - \omega_S)$).

Sometimes the electron spin–spin correlation function of Eq. (5) is expressed in the Heisenberg picture with explicit time-dependent spin operators or in the Schrödinger picture, in terms of the spin density matrix element. Of course these descriptions are equivalent $\langle S_1^{1\dagger}(t) S_1^1(0)\rangle \equiv \langle S_1^{1\dagger} S_1^1\rangle \rho_1^1(t)$. The first rank electron spin density matrix element $\rho_1^1(t)$ represents the time-dependent transverse magnetization. Recently, this relation between NMRD and ESR was questioned by Sharp and Lohr [20].

2.1. The $\mathcal{L}_S$ in GSBM

In Eq. (4), the Liouville superoperator $\mathcal{L}_S$ governing the electron spin correlation function reads

$$\mathcal{L}_S = \mathcal{L}_S^{\mathrm{Zeeman}} + i\mathcal{R}_{\mathrm{ZFS}}, \tag{6}$$

where $\mathcal{L}_S$ is composed of a Zeeman term and the Redfield superoperator. The latter is generated by the time-dependent ZFS interaction. The Zeeman Hamiltonian is

$$H_S^{\mathrm{Zeeman}} = -\hbar\gamma_S B_0 S_0^1, \tag{7}$$

where $\gamma_S = \frac{g_e}{2} 1.76084 \times 10^{11}\ \mathrm{rads}^{-1} T^{-1}$. The spectral density s_σ^{DD} in Eq. (4) may be extracted as a matrix element, $M_{\sigma\sigma}^{-1}$ of the inverted full matrix $\mathcal{M}$, generated by the Liouville and Redfield superoperators (cf. Eq. (6)). The explicit expressions for the inverted matrix element, s_1^{DD}, are given by Eq. (A.6) in Appendix A and s_0^{DD} in Eq. (B.4) of Appendix B.

2.2. The $\mathcal{L}_S$ in the SLA

In the stochastic Liouville approach (SLA), the full Liouville operator Eq. (6) is replaced by

$$\mathcal{L}_S = \mathcal{L}_S^{\mathrm{Zeeman}} + \mathcal{L}_S^{\mathrm{ZFS}}(\Omega) + i\Gamma_{PR}(\Omega). \tag{8}$$

Here, $\mathcal{L}_S^{\mathrm{Zeeman}}$, $\mathcal{L}_S^{\mathrm{ZFS}}(\Omega)$, and $\Gamma_{PR}(\Omega)$ stand for the electron spin Zeeman Liouvillean, the stochastic time-dependent ZFS interaction, and the Markov operator, respectively. The latter describes the dynamics of the relevant stochastic variables Ω of the ZFS interaction [16,17].

In the Liouville space, one may construct a supermatrix of infinite dimension: $\mathcal{M}_{\mathcal{L}} = -i\mathcal{L}_{\mathbf{S}} + (i\omega_I + \frac{1}{\tau_R})\mathbf{E}$ where $\mathbf{E}$ is the unit matrix. We have indicated, with an index (L), that this matrix should not be mixed up with the M matrices of the GSBM theory given in the appendices. In Liouville space, the matrix elements of $\mathcal{L}_{\mathbf{S}}$ are $\mathbf{L}_{\mathbf{ij}} \equiv (O_i^\dagger|L_S|O_j) = \mathrm{tr}_L\{O_i^\dagger[H_S, O_j]\}$, expressed in terms of the commutator and a complete set of operators $|O_j)$ spanning the Liouville space. The basis operator $|O_j)$ refers to the direct product of spin operators and eigenfunctions to the diffusion operator Γ_{PR}, describing the classical degrees of freedom. In the appendices of the review article [17] and in the papers [18,19], the construction of this Liouville matrix is given in more detail. Again the spectral density, s_n^{DD} is obtained from a matrix inversion,

$$s_n^{\mathrm{DD}}(\omega_I) = c_n^* \mathcal{M}_{\mathcal{L}}^{-1} c_n, \tag{9}$$

where vector c_n projects out the relevant matrix elements of the full inverted supermatrix matrix $\mathcal{M}_{\mathcal{L}}^{-1}$.

3. Results and discussion

In this section, we present a number of NMRD profile and ESR lineshape calculations to determine the

range of validity for GSBM. The parameters used for the different calculations displayed in the figures are summarized in Table 1.

Fig. 1 displays the theoretical NMRD profiles and the X-, W-band ESR spectra obtained using GSBM and SLA for the best-fit ZFS parameters of the Gd(III) MS-325 + HSA complex [10]. The GSBM theory could reproduce the NMRD profile well, but we noticed a significant discrepancy between the theoretical ESR lineshape and the recorded X-band spectrum. The parameters extracted indicate that the perturbation approach should be applicable, provided that a static ZFS interaction is sufficiently small. The ZFS interaction obtained from fitting the NMRD profile was relatively small $\Delta_{ZFS} = 0.018\ \mathrm{cm}^{-1}$ resulting in $\Delta_{ZFS}\tau_f = 0.1$, which is smaller than 1, but not very much smaller, which is generally required for a second-order perturbation approach. If there is a "static" ZFS interaction, it must be much smaller than the transient ZFS, because the reorientational correlation time, $\tau_R = 10^{-8}$ s, is so large [10]. A correlation time of $\tau_f = 30$ ps indicates non-extreme narrowing conditions, $\omega_S\tau_f > 1$, and thus multi-exponential electron spin relaxation is expected. A very small discrepancy between the NMRD profiles obtained from GSBM and SLA is shown in Fig. 1. The NMRD profiles actually coincide over the whole range of magnetic fields. The X-band and W-band spectra of Fig. 1 calculated using the GSBM lineshape function are also very similar to those of the SLA approach.

The NMRD profiles and ESR spectra calculated using parameters which corresponds to small Gd(III) complexes, such as MS-325 or Gd-DTPA and others, are displayed in Fig. 2. The extreme narrowing condition prevails for the electron spin system and the reorientational correlation time $\tau_R = 74$ ps is the range for most small size contrast agents. The GSBM theory and SLA give almost identical results for NMRD profiles and ESR spectra.

Fig. 3 refers to a case where the second-order perturbation approach breaks down. The interaction strength parameter, $\Delta_{ZFS} \cdot \tau_f = 0.603$ is clearly outside the regime of validity for second-order perturbation theory. The correlation time of $\tau_f = 10$ ps implies extreme narrowing

Table 1
Parameters used for both theories in NMRD and ESR X-, W-band calculation

Figure	Δ_{ZFS} (cm^{-1}/rad s^{-1})	τ_f (ps)	$\Delta_{ZFS} \cdot \tau_f$	τ_R (ps)
Fig. 1	$0.018/0.339 \times 10^{10}$	30	0.102	10000
Fig. 2	$0.04/0.754 \times 10^{10}$	9	0.068	74
Fig. 3	$0.32/6.032 \times 10^{10}$	10	0.603	74
Fig. 4	$0.091/1.714 \times 10^{10}$	30	0.514	433
Fig. 5	$0.038/0.716 \times 10^{10}$	150	1.07	—

Notice that τ_R is not involved in ESR calculation for both GSBM and SLA methods.

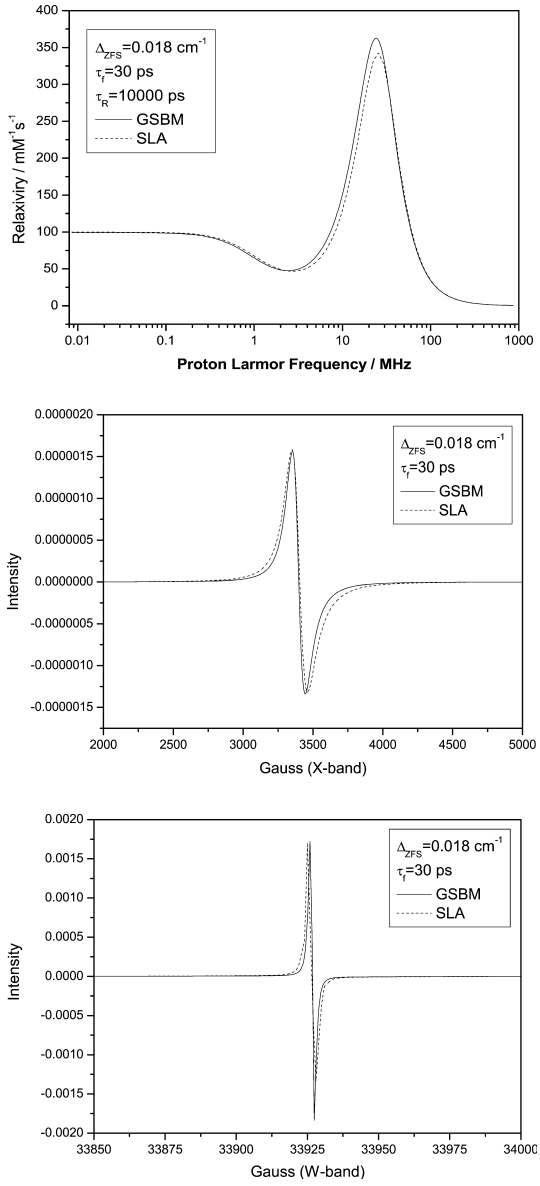

Fig. 1. Calculated NMRD profiles and X-, W-band ESR lineshapes of both theories using parameters in Table 1. $\Delta_{ZFS} = 0.018\ \mathrm{cm}^{-1}$, $\tau_f = 30$ ps, $\tau_R = 10000$ ps. Solid line is from GSBM theory and scattered line is from SLA.

conditions for the electron spin system. The low-field region of the NMRD profile calculated using GSBM is significantly underestimated, whereas the high-field region is still satisfactorily described. However, the X-band ESR spectra of GSBM and SLA are clearly different. The GSBM displays a Lorentzian lineshape, whereas the SLA displays a slow-motion-like spectrum that exhibits an interesting wave-like character in the wings. The W-band ESR spectra are more like the GSBM Lorentzian lineshape but SLA generates a significantly broader linewidth.

In Fig. 4, we have changed the condition as compared to Fig. 3 by increasing the correlation time $\tau_f = 30$ ps,

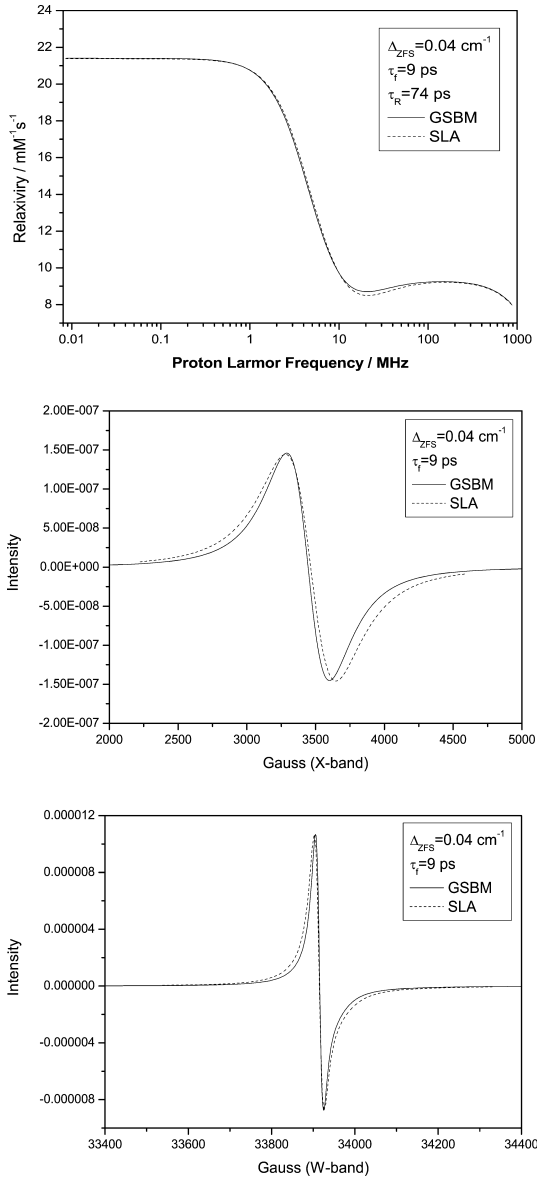

Fig. 2. Calculated NMRD profiles and X-, W-band ESR lineshapes of both theories using parameters in Table 1. $\Delta_{ZFS} = 0.04\ cm^{-1}$, $\tau_f = 9$ ps, $\tau_R = 74$ ps. Solid line is from GSBM theory and scattered line is from SLA.

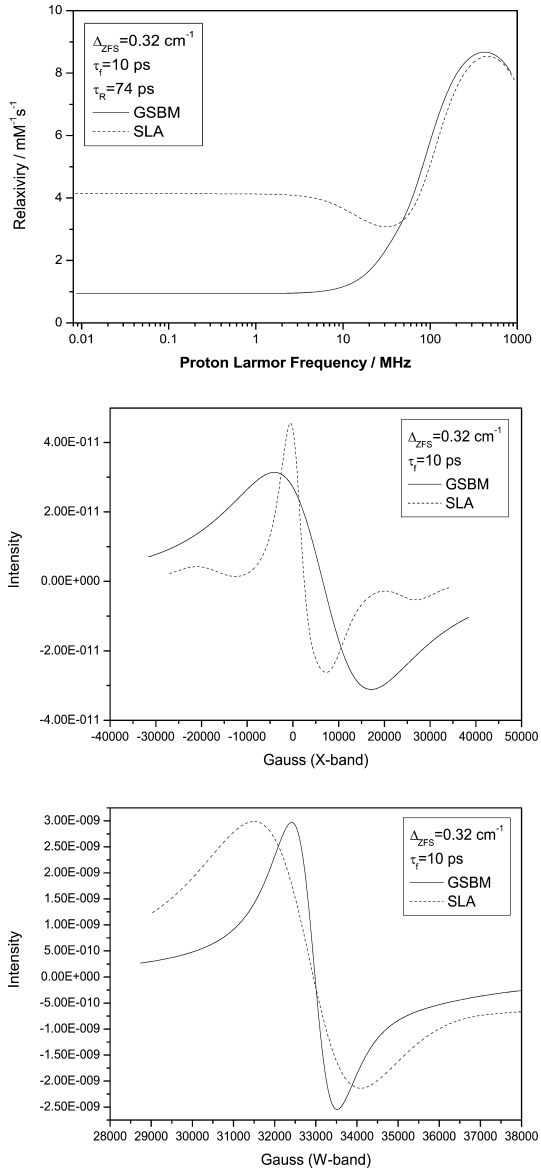

Fig. 3. Calculated NMRD profiles and X-, W-band ESR lineshapes of both theories using parameters in Table 1. $\Delta_{ZFS} = 0.32\ cm^{-1}$, $\tau_f = 10$ ps, $\tau_R = 74$ ps. Solid line is from GSBM theory and scattered line is from SLA.

implying non-extreme narrowing conditions. The GSBM theory breaks down and SLA produces an interesting X-band spectrum. The X-band spectra in Figs. 3 and 4 are similar in showing a non-Lorentzian lineshape with wave-like wings. Both X-band curves show similar character in the low-field wing as the experimental X-band spectrum of MS-325 + HSA. The high-field wing of X-band in Fig. 4 is, however, too pronounced.

One has to be aware that the negative values of magnetic fields of the ESR X-band spectra in Figs. 3 and 4 are not physically possible. In the range 1000–6000 G, our analytical lineshape function cannot give the full X-band ESR spectra because the linewidth is too broad. However, mathematically it is possible to use negative magnetic field values in our lineshape function to give full spectra.

In Fig. 5, we display the experimental X-band ESR lineshape of MS-325 + HSA (solid line). The dash line represents the slow-motion spectrum calculated using SLA, which has a characteristic low-field shoulder, and the asymmetric intensity with the wave-like character in the high-field wings. This lineshape conforms quite well with the non-Lorentzian character of the X-band ESR lineshape of MS-325 + HSA. The ZFS interaction used $\Delta_{ZFS} = 0.038\ cm^{-1}$ which indicates a significantly larger ZFS interaction than was used to reproduce the NMRD profile. The correlation time $\tau_f = 150$ ps cannot

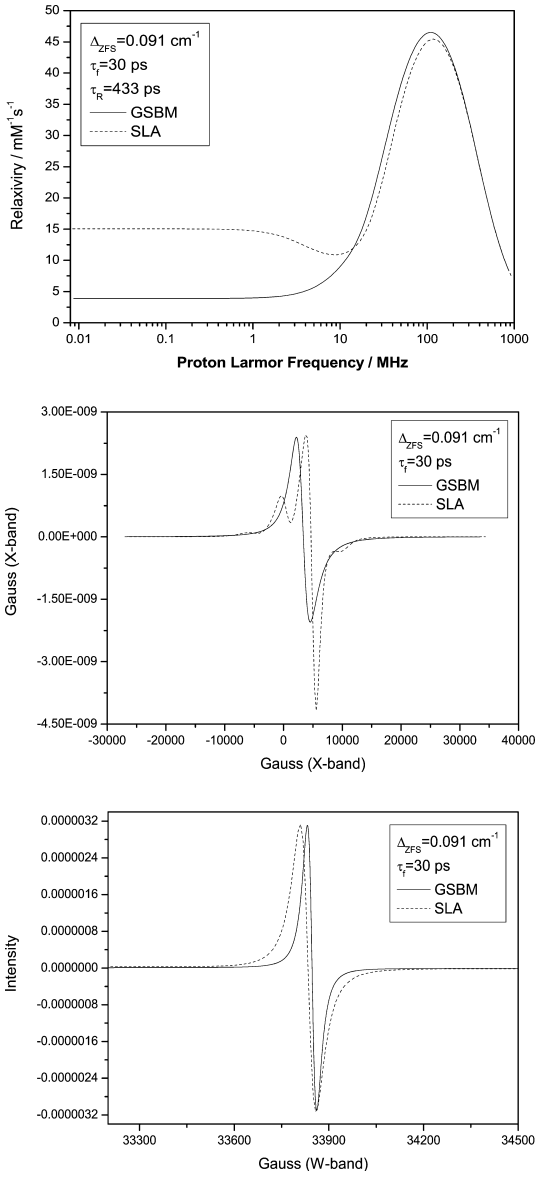

Fig. 4. Calculated NMRD profiles and X-, W-band ESR lineshapes of both theories using parameters in Table 1. $\Delta_{\mathrm{ZFS}} = 0.091\ \mathrm{cm}^{-1}$, $\tau_f = 30$ ps, $\tau_{\mathrm{R}} = 433$ ps. Solid line is from GSBM theory and scattered line is from SLA.

be the reorientational correlation time of the whole complex but should be interpreted as a very slow "distortional correlation time." We have not been able to resolve the nature of this dynamics. The dynamics model used in this work can only indicate slow-motion conditions. The simple two dynamics model includes a fast dynamics, characterized by a distortional correlation time (1–10 ps) and a slow diffusion process which in most cases refers to the motion of the whole complex. This finding seems to indicate that the transient ZFS must include at least two different time scales.

A detailed analysis of this case requires more ESR and NMRD experiments and a refined dynamics model

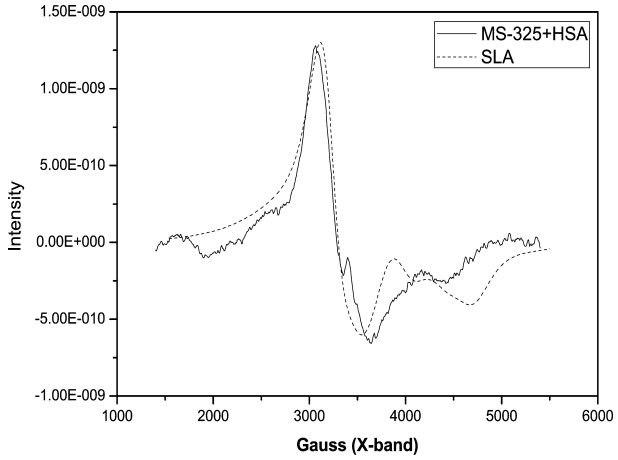

Fig. 5. X-band ESR lineshapes of MS-325 + HSA. Solid line is from experiment and dash line is from SLA calculation where $\Delta_{\mathrm{ZFS}} = 0.038\ \mathrm{cm}^{-1}$, $\tau_f = 150$ ps, and $\Delta_{\mathrm{ZFS}} \cdot \tau_f = 1.07$.

of the ZFS interaction. Here, we only want to indicate that this rather strange X-band lineshape seems to be a slow-motion spectrum. The interaction strength parameter, $\Delta_{\mathrm{ZFS}} \cdot \tau_f = 1.07$, obviously falls outside the perturbation regime.

For cases with the interaction parameter $\Delta_{\mathrm{ZFS}} \cdot \tau_f \leqslant 0.1$, the GSBM theory reproduces the SLA results very well. The NMRD profiles are nicely reproduced over the whole range of magnetic fields while the different ESR band spectra are fairly well reproduced by the lineshape function $I(\omega_S - \omega)$. We conclude that the GSBM-theory calculates the NMRD profile accurately over the whole range of magnetic fields, provided the interaction parameter satisfies the condition $\Delta_{\mathrm{ZFS}} \cdot \tau_f \leqslant 0.1$.

4. Conclusions

Within the perturbation regime set to $\Delta_{\mathrm{ZFS}} \cdot \tau_f \leqslant 0.1$, the GSBM and SLA theories give very similar results and it is concluded that the GSBM and the ESR lineshape function leads to accurate results. Within the perturbation regime as defined above, the relatively simple GSBM theory is thus a safe tool in analysing both NMRD profiles and ESR spectra.

The rather spectacular X-band lineshape observed for the Gd(III) MS-325 + HSA complex, which could not be reproduced by the GSBM theory, is very likely a slow-motion spectrum. To analyse this X-band spectrum, we need the SLA and probably a more sophisticated dynamics model of the ZFS, which includes more than two different time scales. A careful study using a many dynamics model is needed to resolve the time scale and the nature of the $\tau_f \approx 150$ ps distortion correlation time.

Acknowledgments

Erik Rosenbaum and Professor Lennart Johansson are gratefully acknowledged for linguistic corrections.

Appendix A. The electron spin–spin spectral density s_1^{DD}

The Redfield matrix describing electron spin–spin relaxation for $S = 7/2$ can be represented in Zeeman basis, and if rewrite it with symbols, then we have:

$$\mathbf{R} = \begin{bmatrix} A & B & C & 0 & 0 & 0 & 0 \\ B & D & E & F & 0 & 0 & 0 \\ C & E & G & 0 & H & 0 & 0 \\ 0 & F & 0 & I & 0 & F & 0 \\ 0 & 0 & H & 0 & G & E & C \\ 0 & 0 & 0 & F & E & D & B \\ 0 & 0 & 0 & 0 & C & B & A \end{bmatrix}, \tag{A.1}$$

where the matrix elements are given in the following table.

Matrix elements of $\mathbf{R}(\beta_{LM})$ for $S = 7/2$

$A = 54J_0 + 174J_1 + 66J_2 - \mathrm{i}78Q_1 + \mathrm{i}24Q_2$
$B = -24\sqrt{21}J_1$
$C = -6\sqrt{105}J_2$
$D = 24J_0 + 174J_1 + 126J_2 - \mathrm{i}18Q_1 - \mathrm{i}6Q_2$
$E = -24\sqrt{5}J_1$
$F = -60\sqrt{3}J_2$
$G = 6J_0 + 78J_1 + 186J_2 + \mathrm{i}18Q_1 - \mathrm{i}24Q_2$
$H = -120J_2$
$I = 30J_1 + 210J_2 + \mathrm{i}30Q_1 - \mathrm{i}30Q_2$

Then we add the static ZFS interaction term, defined as

$$H_0^{\mathrm{ZFS}}(\beta_{LM}) = \sqrt{\frac{2}{3}} D_s S_{PM} d_{00}^2(\beta_{LM}) S_0^2, \tag{A.2}$$

where S_{PM} is an order parameter given by $S_{PM} = \langle d_{00}^2(\beta_{PM}) \rangle$. The resulting matrix is then transformed to an irreducible spherical electron spin tensor base with the operator basis set O_σ^Σ

$$O_\sigma^\Sigma = \sum_m \sqrt{2\Sigma+1} \begin{pmatrix} S & S & \Sigma \\ m+\sigma & -m & -\sigma \end{pmatrix} (-1)^{S-m-\sigma} |Sm+\sigma\rangle\langle Sm| \tag{A.3}$$

expressed in terms of Zeeman eigenoperators $|\, Sm+\sigma\rangle\langle Sm\,|$ and where

$$\begin{pmatrix} S & S & \Sigma \\ m+\sigma & -m & -\sigma \end{pmatrix} \tag{A.4}$$

is a 3*j*-symbol [21].

The resulting matrix is written with first even rank tensors and then odd rank tensors, in the order 2, 4, 6, 1, 3, 5, 7. The Zeeman matrix $\mathbf{1}\mathrm{i}(\omega_I \pm \omega_S)$ is then added. We get a matrix of the form

$$\mathbf{M}_{\pm\mathbf{1}} = \begin{bmatrix} a & b & 0 & c & d & 0 & 0 \\ b & e & f & 0 & g & h & 0 \\ 0 & f & i & 0 & 0 & j & k \\ c & 0 & 0 & l & m & 0 & 0 \\ d & g & 0 & m & n & p & 0 \\ 0 & h & j & 0 & p & q & r \\ 0 & 0 & k & 0 & 0 & r & s \end{bmatrix} \tag{A.5}$$

with the elements defined in the table given below.

Matrix elements of $\mathbf{M}_{\pm\mathbf{1}}(\beta_{LM})$ for $S = 7/2$

$a = \frac{6}{7}(43J_0 + 51J_1 + 102J_2 - \mathrm{i}51Q_1 + \mathrm{i}8Q_2) + \mathrm{i}(\omega_I \pm \omega_S)$

$b = \frac{12\sqrt{110}}{7}(J_0 + 2J_1 - 3J_2 - \mathrm{i}2Q_1 + \mathrm{i}Q_2)$

$c = 2\sqrt{3} D_s S_{PM} d_{00}^2(\beta_{LM})$

$d = 2\sqrt{\frac{22}{7}} D_s S_{PM} d_{00}^2(\beta_{LM})$

$e = \frac{6}{77}(402J_0 + 2281J_1 + 2707J_2 - \mathrm{i}419Q_1 + \mathrm{i}17Q_2) + \mathrm{i}(\omega_I \pm \omega_S)$

$f = \frac{42\sqrt{10}}{11}(J_0 + 8J_1 - 9J_2 - \mathrm{i}2Q_1 + \mathrm{i}Q_2)$

$g = 4\sqrt{\frac{5}{7}} D_s S_{PM} d_{00}^2(\beta_{LM})$

$h = 2\sqrt{\frac{26}{11}} D_s S_{PM} d_{00}^2(\beta_{LM})$

$i = \frac{6}{11}(29J_0 + 375J_1 + 366J_2 - \mathrm{i}3Q_1 - \mathrm{i}26Q_2) + \mathrm{i}(\omega_I \pm \omega_S)$

$j = 14\sqrt{\frac{5}{143}} D_s S_{PM} d_{00}^2(\beta_{LM})$

$k = 4\sqrt{\frac{3}{13}} D_s S_{PM} d_{00}^2(\beta_{LM})$

$l = 6\,(3J_0 + 5J_1 + 2J_2 - \mathrm{i}Q_1 - \mathrm{i}2Q_2) + \mathrm{i}(\omega_I \pm \omega_S)$

$m = 6\sqrt{\frac{66}{7}}(J_0 - J_2 - \mathrm{i}2Q_1 + \mathrm{i}Q_2)$

$n = 2\,(18J_0 + 55J_1 + 77J_2 - \mathrm{i}21Q_1 + \mathrm{i}3Q_2) + \mathrm{i}(\omega_I \pm \omega_S)$

$p = 4\sqrt{\frac{130}{77}}(3J_0 + 14J_1 - 17J_2 - \mathrm{i}6Q_1 + \mathrm{i}3Q_2)$

$q = \frac{2}{13}(159J_0 + 1427J_1 + 1534J_2 - \mathrm{i}123Q_1 - \mathrm{i}36Q_2) + \mathrm{i}(\omega_I \pm \omega_S)$

$r = \frac{84}{143}\sqrt{165}(J_0 + 12J_1 - 13J_2 - \mathrm{i}2Q_1 + \mathrm{i}Q_2)$

$s = \frac{6}{13}(12J_0 + 209J_1 + 143J_2 + \mathrm{i}41Q_1 - \mathrm{i}53Q_2) + \mathrm{i}(\omega_I \pm \omega_S)$

The element s_1^{DD} we are interested in is the (4,4) matrix element of the inverted matrix $M_{\pm 1}^{-1}$:

$$s_1^{\mathrm{DD}} = \frac{X}{Y}, \tag{A.6}$$

where $X = (k^2nb^2q + eak^2p^2 - eak^2qn - asnf^2q + 2\,asnjfh - 2\,aspfgj + asg^2j^2 + asf^2p^2 - 2\,dsgbj^2 + sb^2j^2n + 2\,dspfbj -$

$2\ d^2sjfh + ieasnq + 2\ idsgbq - 2\ idr^2gb - \ iash^2n + 2\ iasphg - 2\ idsphb - isb^2nq - ieasp^2 - iear^2n - \ ied^2sq - iasg^2q + id^2er^2 + iar^2g^2 + ir^2b^2n + id^2sh^2 - easj^2n + ed^2sj^2 + isb^2p^2 + d^2sf^2q - d^2k^2h^2 - 2\,kjnb^2r - 2\,arkjg^2 - 2\,ak^2phg + 2\ d^2kfhr - 2\ d^2erkj - 2\ dk^2qgb + 2\ earkjn + 2\ arfkpg + d^2ek^2q + 4\ \ dkjgbr - 2\ \ dfkpbr - d^2r^2f^2 + 2\ \ dk^2phb + ak^2h^2n - 2\ \ \ akfhrn + ak^2qg^2 + ar^2f^2n - k^2p^2b^2)$ and $Y = (-r^2nc^2f^2 - sf^2p^2c^2 - sc^2j^2g^2 - ar^2m^2f^2 - k^2qb^2m^2 - k^2c^2h^2n - sb^2m^2j^2 - k^2c^2qg^2 + 4derkjmc - 2\ desj^2mc - 2\ dsmcf^2q + iear^2m^2 + lk^2nb^2q + lar^2f^2n + lasg^2j^2 + ld^2sf^2q + ier^2nc^2 + iesc^2p^2 + isb^2m^2q - 2\,asm^2jfh + 2\,k^2qmbcg - 2\ spbcmfj + 2\ akfhrm^2 - ak^2h^2m^2 + iasm^2h^2 + isc^2h^2n + isc^2qg^2 + 2\ \ ispbcmh + 2\ \ ir^2gbmc - isc^2phg - iesc^2qn - ieasm^2q - 2\,ismbcgq - 2\,idsh^2mc + ilsb^2p^2 + 2\,idesmcq - 2\ \ ider^2mc + ilr^2b^2n - ilasg^2q - ilsb^2nq + 2\ \ ilasphg - 2\ ildsphb\ -\ 2\ \ ildr^2gb\ +\ ilar^2g^2\ -\ ild^2esq + 2\ \ ildsgbq + ileasnq - ileasp^2 - ilear^2n - ilash^2n + ild^2er^2 + ild^2sh^2 + 2\,fkpbrmc + asm^2f^2q + 2\,sc^2pfgj + 2\,kfhrnc^2 + 2\,rb^2m^2kj - 4\ kjgbrmc + 2\ \ sgbj^2mc + 2\ \ k^2c^2phg + ek^2c^2qn + esc^2j^2n + easm^2j^2 - 2\,earkjm^2 + eak^2m^2q - 2\,erkjnc^2 - 2\,k^2pbcmh + 2\,rkjg^2c^2 - ek^2c^2p^2 - 2sc^2jfhn - 2\,rfkpgc^2 + sf^2qnc^2 - 2\ dek^2qmc + 2\ \ dr^2f^2mc + 2\ \ dk^2h^2mc - 4\ \ dkfhrmc + 4\ dsmcjfh - ir^2b^2m^2 - lk^2p^2b^2 - ld^2k^2h^2 + lasf^2p^2 - \ leak^2qn - 2\ \ lakfhrn + 2\ \ ldk^2phb - 2\ \ ldfkpbr + 2\ \ ldspfbj + 4\ ldkjgbr - 2\ \ \ \ ldsgbj^2 + lak^2qg^2 + lak^2h^2n + lsb^2j^2n + leak^2p^2 + ld^2ek^2q + ld^2esj^2 - leasj^2n + 2\ learkjn - ld^2r^2f^2 + 2\ \ larfkpg - 2\ \ ldk^2qgb + 2\ \ ld^2kfhr - 2\ \ ld^2erkj - 2\ ld^2sjfh + 2\ \ lasnjfh - lasnf^2q - 2\ \ lak^2phg - 2\ \ larkjg^2 - 2\ laspfgj - 2\,lkjnb^2r - ir^2g^2c^2)$.

Appendix B. The electron spin–lattice spectral density s_0^{DD}

Again we start with the Redfield matrix describing electron spin–lattice relaxation. The Zeeman basis is given in symbolic form

$$\mathbf{R} = \begin{bmatrix} A & B & C & 0 & 0 & 0 & 0 & 0 \\ B & D & E & F & 0 & 0 & 0 & 0 \\ C & E & G & H & I & 0 & 0 & 0 \\ 0 & F & H & J & 0 & I & 0 & 0 \\ 0 & 0 & I & 0 & J & H & F & 0 \\ 0 & 0 & 0 & I & H & G & E & C \\ 0 & 0 & 0 & 0 & F & E & D & B \\ 0 & 0 & 0 & 0 & 0 & C & B & A \end{bmatrix}, \tag{B.1}$$

where the matrix elements are given in the table below.

Matrix elements of $\mathbf{R}(\beta_{LM})$ for $S = 7/2$

$A = 126J_1 + 42J_2$	$G = 126J_1 + 162J_2$
$B = -126J_1$	$H = -30J_1$
$C = -42J_2$	$I = -120J_2$
$D = 222J_1 + 90J_2$	$J = 30J_1 + 210J_2$
$E = -96J_1$	
$F = -90J_2$	

Then we transform the basis using the similar method as previous part. In this case, the static ZFS interaction term is zero. The transformed matrix has the following form:

$$\mathbf{N} = \begin{bmatrix} 0 & 0 & 0 & 0 & 0 & 0 & 0 & 0 \\ 0 & A & 0 & H & 0 & 0 & 0 & 0 \\ 0 & 0 & B & 0 & I & 0 & 0 & 0 \\ 0 & H & 0 & C & 0 & J & 0 & 0 \\ 0 & 0 & I & 0 & D & 0 & K & 0 \\ 0 & 0 & 0 & J & 0 & E & 0 & L \\ 0 & 0 & 0 & 0 & K & 0 & F & 0 \\ 0 & 0 & 0 & 0 & 0 & L & 0 & G \end{bmatrix}. \tag{B.2}$$

The above matrix can be reduced to a 4×4 matrix since only odd-rank tensor operators enter the theoretical description. The final $\mathbf{M}_0$ matrix is formed as

$$\mathbf{M_0} = \begin{bmatrix} a & e & 0 & 0 \\ e & b & f & 0 \\ 0 & f & c & g \\ 0 & 0 & g & d \end{bmatrix}, \tag{B.3}$$

where the matrix elements are given in the table below.

Matrix elements of $\mathbf{M}_1(\beta_{LM})$ for $S = 7/2$

$a = 12(J_1 + 4J_2) - \mathrm{i}\omega_I + \frac{1}{\tau_R}$
$b = 12(12J_1 + 13J_2) - \mathrm{i}\omega_I + \frac{1}{\tau_R}$
$c = \frac{60}{13}(53J_1 + 51J_2) - \mathrm{i}\omega_I + \frac{1}{\tau_R}$
$d = \frac{168}{13}(8J_1 + 5J_2) - \mathrm{i}\omega_I + \frac{1}{\tau_R}$
$e = 24\sqrt{\frac{11}{7}}(J_1 - J_2)$
$f = 240\sqrt{\frac{13}{77}}(J_1 - J_2)$
$g = \frac{240}{13}\sqrt{\frac{343}{11}}(J_1 - J_2)$

The inverted matrix element is given by

$$s_0^{DD} = \frac{bcd - df^2 - bg^2}{abcd - cde^2 - adf^2 - abg^2 + e^2g^2}. \tag{B.4}$$

Appendix C. The ESR lineshape function

The derivation of ESR lineshape function has the same procedure as that in the part of electron spin–spin spectral density. The differences are the definition of the **M** matrix and $\sigma = 1$. The matrix elements are given in the following table.

$$I(\omega) = \frac{X}{Y}, \tag{C.1}$$

where X and Y have the same expression as in Eq. (A.6).

ESR lineshape matrix elements, $\sigma = 1$

$a = \frac{6}{7}(43J_0 + 51J_1 + 102J_2 - \mathrm{i}51Q_1 + \mathrm{i}8Q_2) + \mathrm{i}(\omega + \omega_S)$
$b = \frac{12\sqrt{110}}{7}(J_0 + 2J_1 - 3J_2 - \mathrm{i}2Q_1 + \mathrm{i}Q_2)$
$c = 2\sqrt{3}D_s S_{PM} d^2_{00}(\beta_{LM})$
$d = 2\sqrt{\frac{22}{7}}D_s S_{PM} d^2_{00}(\beta_{LM})$
$e = \frac{6}{77}(402J_0 + 2281J_1 + 2707J_2 - \mathrm{i}419Q_1 + \mathrm{i}17Q_2) + \mathrm{i}(\omega + \omega_S)$
$f = \frac{42\sqrt{10}}{11}(J_0 + 8J_1 - 9J_2 - \mathrm{i}2Q_1 + \mathrm{i}Q_2)$
$g = 4\sqrt{\frac{5}{7}}D_s S_{PM} d^2_{00}(\beta_{LM})$
$h = 2\sqrt{\frac{26}{11}}D_s S_{PM} d^2_{00}(\beta_{LM})$
$i = \frac{6}{11}(29J_0 + 375J_1 + 366J_2 - \mathrm{i}3Q_1 - \mathrm{i}26Q_2) + \mathrm{i}(\omega + \omega_S)$
$j = 14\sqrt{\frac{5}{143}}D_s S_{PM} d^2_{00}(\beta_{LM})$
$k = 4\sqrt{\frac{3}{13}}D_s S_{PM} d^2_{00}(\beta_{LM})$
$l = 6\,(3J_0 + 5J_1 + 2J_2 - \mathrm{i}Q_1 - \mathrm{i}2Q_2) + \mathrm{i}(\omega + \omega_S)$
$m = 6\sqrt{\frac{66}{7}}(J_0 - J_2 - \mathrm{i}2Q_1 + \mathrm{i}Q_2)$
$n = 2\,(18J_0 + 55J_1 + 77J_2 - \mathrm{i}21Q_1 + \mathrm{i}3Q_2) + \mathrm{i}(\omega + \omega_S)$
$p = 4\sqrt{\frac{130}{77}}(3J_0 + 14J_1 - 17J_2 - \mathrm{i}6Q_1 + \mathrm{i}3Q_2)$
$q = \frac{2}{13}(159J_0 + 1427J_1 + 1534J_2 - \mathrm{i}123Q_1 - \mathrm{i}36Q_2) + \mathrm{i}(\omega + \omega_S)$
$r = \frac{84}{143}\sqrt{165}(J_0 + 12J_1 - 13J_2 - \mathrm{i}2Q_1 + \mathrm{i}Q_2)$
$s = \frac{6}{13}(12J_0 + 209J_1 + 143J_2 + \mathrm{i}41Q_1 - \mathrm{i}53Q_2) + \mathrm{i}(\omega + \omega_S)$

References

[1] P. Caravan, N.J. Cloutier, M.T. Greenfield, S.A. McDermid, S.U. Dunham, J.W.M. Bulte, J.C. Amedio Jr., R.J. Looby, R.M. Supkowski, W.D. Horrocks Jr., T.J. McMurry, R.B. Lauffer, The interaction of MS-325 with human serum albumin and its effect on proton relaxation rates, J. Am. Chem. Soc. 124 (2002) 3152–3162.

[2] I. Solomon, Relaxation processes in a system of two spins, Phys. Rev. 99 (1955) 559–565.

[3] N. Bloembergen, Proton relaxation times in paramagnetic solutions, J. Chem. Phys. 27 (1957) 572–573.

[4] N. Bloembergen, L.O. Morgan, Proton relaxation times in paramagnetic solutions: effects of electron spin relaxation, J. Chem. Phys. 34 (1961) 842–850.

[5] C.P. Slichter, Principles of Magnetic Resonance, third ed., Springer-Verlag, Heidelberg, Germany, 1990.

[6] M. Rubenstein, A. Baram, Z. Luz, Electronic and nuclear relaxation in solutions of transition metal ions with spin $S = 3/2$ and 5/2, Mol. Phys. 20 (1971) 67–80.

[7] P.-O. Westlund, A generalized Solomon–Bloembergen–Morgan theory for arbitrary electron spin quantum number S. The dipole–dipole coupling between a nuclear spin $I = 1/2$ and an electron spin system $S = 5/2$, Mol. Phys. 85 (1995) 1165–1178.

[8] E. Strandberg, P.-O. Westlund, 1H NMRD profile and ESR lineshape calculation for an isotropic electron spin system with $S = 7/2$. A generalized modified Solomon–Bloembergen–Morgan theory for nonextreme-narrowing conditions, J. Magn. Reson. Ser. A 122 (1996) 179–191.

[9] E. Strandberg, P.-O. Westlund, Paramagnetic proton nuclear spin relaxation theory of low-symmetry complexes for electron spin quantum number $S = 5/2$, J. Magn. Reson. 137 (1999) 333–344.

[10] X. Zhou, P. Caravan, R.B. Clarkson, P.-O. Westlund, On the philosophy of optimizing contrast agents. An analysis of 1H NMRD profiles and ESR lineshapes of the Gd(III)complex MS-325 + HSA, J. Magn. Reson. 167 (2004) 147–160.

[11] P.H. Fries, G. Ferrante, E. Belorizky, S. Rast, The rotational motion and electronic relaxation of the Gd(III) aqua complex in water revisited through a full proton relaxivity study of a probe solute, J. Chem. Phys. 119 (2003) 8636–8644.

[12] S. Rast, P.H. Fries, E.J. Belorizky, Theoretical study of electronic relaxation processes in hydrated Gd(III) complexes in solutions, J. Chim. Phys. 96 (1999) 1543–1550.

[13] S. Rast, A. Borel, L. Helm, E. Belorizky, P.H. Fries, A.E. Merbach, EPR spectroscopy of MRI-related Gd(III) complexes: simultaneous analysis of multiple frequency and temperature spectra, including static and transient crystal field effects, J. Am. Chem. Soc. 123 (2001) 2637–2644.

[14] S. Rast, P.H. Fries, E.J. Belorizky, Static zero field splitting effects on the electronic relaxation of paramagnetic metal ion complexes in solution, J. Chem. Phys. 113 (2000) 8724–8735.

[15] P.-O. Westlund, N. Benetis, H. Wennerström, Paramagnetic proton nuclear magnetic relaxation in the Ni^{2+} hexaquo complex: a theoretical study, Mol. Phys. 61 (1987) 177–194.

[16] J. Kowalewski, L. Nordenskiöld, N. Benetis, P.-O. Westlund, Theory of nuclear spin relaxation in paramagnetic system in solution, Prog. NMR Spectrosc. 17 (1985) 141–185.

[17] P.-O. Westlund, in: J.J. Delpuech (Ed.), Dynamics of Solutions and Fluid Mixtures by NMR, Wiley, New York, 1995, Chapter 4.

[18] T. Nilsson, J. Svoboda, P.-O. Westlund, J. Kowalewski, Slow-motion theory of nuclear spin relaxation in paramagnetic complexes ($S = 1$) of arbitrary symmetry, J. Chem. Phys. 109 (1998) 6364–6374.

[19] T. Larsson, P.-O. Westlund, J. Kowalewski, S.H. Koenig, Nuclear-spin relaxation in paramagnetic complexes in the slow-motion regime for the electron spin: the anisotropic pseudorotation model for $S = 1$ and the interpretation of nuclear magnetic relaxation dispersion results for a low-symmetry Ni(II) complex, J. Chem. Phys. 101 (1994) 1116–1128.

[20] R. Sharp, L. Lohr, Thermal relaxation of electron spin motion in a thermal equilibrium ensemble: relation to paramagnetic nuclear magnetic resonance relaxation, J. Chem. Phys. 115 (2001) 5005–5014.

[21] D.M. Brink, G.R. Satchler, Angular Momentum, Oxford University Press, Oxford, 1968.